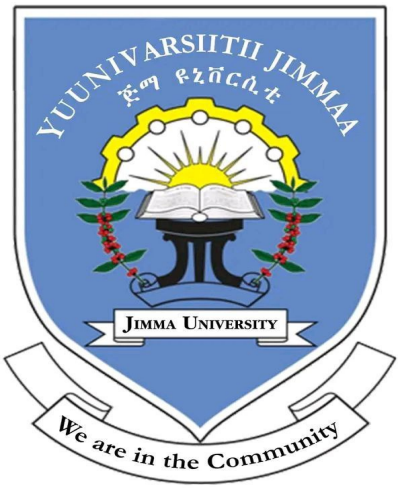

FIRST PRINCIPLE CALCULATION OF STRUCTIONAL AND ELECTRONIC PROPERTIES OF $BiFeO_3$ USING QUANTUM ESPRESSO PACKAGE

By:

Pal Gatluak Deng

A THESIS SUBMITTED TO THE GRADUATE STUDIES OF JIMMA UNIVERSITY IN PARTIAL FULFILLMENT OF THE REQUIREMENTS FOR THE DEGREE OF MASTER OF SCIENCE IN PHYSICS (CONDENSED MATTER PHYSICS)

Jimma University

Jimma, Ethiopia

June 28, 2024

APPROVAL SHEET

JIMMA UNIVERSITY

COLLEGE OF NATURAL SCIENCE

DEPARTMENT OF PHYSICS

As advisor(s)/Examiner, I/We here certify that I/We have read the thesis prepared by Pal Gatluak under my/our guidance, which is entitled **FIRST PRINCIPLE CALCULATION OF STRUCTIONAL AND ELECTRONIC PROPERTIES OF $BiFeO_3$ USING QUANTUM ESPRESSO PACKAGE**, in its final form and have found that its format, citations and bibliographical style are consistent and acceptable and fulfill the university and department style requirements.

Prof. Menberu Mengesha (PhD)	————	————————
Advisor	Signature	Date
Dr. Nebiyu Gemechu (PhD)	————	————————
Co-advisor	Signature	Date
Dr. Tolu Beressa (PhD)	————	————————
Head of Department	Signature	Date
Dr. Tolu Beressa (PhD)	————	————————
Examiner	Signature	Date

DECLARATION

JIMMA UNIVERSITY
COLLEGE OF NATURAL SCIENCE
DEPARTMENT OF PHYSICS

I here by declare that this MSc thesis is my original work and has not been presented for a degree in any other university, and that all sources of material used for the thesis have been duly acknowledged.

AUTHOR: PAL GATLUAK DENG
TITLE: FIRST PRINCIPLE CALCULATION OF STRUCTIONAL AND ELECTRONIC PROPERTIES OF $BiFeO_3$ USING QUANTUM ESPRESSO PACKAGE
DEPARTMENT: Physics
DEGREE: M.Sc. Convocation: June 28, 2024

Permission is herewith granted to Jimma University to circulate and to have copied for non-commercial purposes, at its discretion, the above title upon the request of individuals or institutions.

Pal Gatluak Deng ———— ————————————
Author Signature Date

Acknowledgment

First of all, I would like to thank my Almighty God. Secondly I would like to express my deep gratitude to my advisor **Prof. Menberu Mengesha (PhD)** for his valuable, intellectual, constructive and meaningful suggestions and valuable encouragement starting from the planning up to the development of this thesis work his outstanding advice, extreme supporting for his effortful and consistent advice were remembered ever. I thank him a lot for his guidance to the right thesis direction.

Lastly many thanks go to my families for their great support and encouragement in all aspects from start to end of this thesis work I would like to acknowledge Jimma University and all my instructors and staffs of Physics and also I would like to extend my thank to my sponsor Gambella Teachers' Educational and Healths Science College for the contribution in my study. Finally, I'm also very grateful to all my lovely parents and friends include my wife **Mer Riek Malow**.

Contents

List of Figures

List of Tables

Abbreviation and Acronym

BiFeO3:-Bismuth Ferrite

Cp:-Carpirandello.

DFT:-Density Functional Theory

E[cut]:-cutoff energy

E[n]:-Electronic energy

eV:-electron Volt

GGA:-Generalized Gradient Approximation

KS:-Kohn Sham

LDA:-Local Density Approximation

OPW:-Orthogonal plane-Wave

PW:-Plane-Wave

PWscf:-Plane-wave self-consistent field

VASP:-Vienna Ab Initio Simulation package

Abstract

The Structural and electronic Properties of Bismuth Ferrite ($BiFeO_3$) was investigated with density functional theory (DFT) using Quantum Espresso package. Our study was based on Density Functional Theory (DFT) with the Perdew-Burke-Ernzerhof (PBE) exchange-correlation functional, Vanderbilt (Norm-conserving) pseudo potentials and the plane wave basis set implemented in the Quantum-ESPRESSO package. The calculation of the total minimum energy and the total minimum force of $BiFeO_3$ was calculated as a function of cutoff energy and K-points sampling. The total minimum energy per cell is monotonically decreasing with increasing cutoff energy due to variational principle. However, this trend can not be predicted from increasing the k-points sampling. The energy cut-off (90 Ry) and k-point grid (5x5x5) valued from total minimum energy convergence test. The computational value of the equilibrium lattice constant is 10.0 Bohr. This result is nearly in good agreement with experimental value is 10.2569 Bohr, with the experimental result of percentage error of 2.4%. In addition to this the band structure and total density of state are calculated. From the band structure it is observed that the band gap value is under estimated as compared to the experimental band gap value and the band gap of bismuth ferrite ($BiFeO_3$) is 1.68 eV.

Keywords: Bismuth Ferrite, Density Functional Theory, Electronic and structural properties Bismuth Ferrite ($BiFeO_3$) .

1

Introduction

1.1 General Back Ground of the Study

Bismuth ferrite (BFO) is one of the promising multiferroic materials due to its unique properties such as high Curie and Neel temperatures non toxicity and hence has received intense research interest during the past decade.

Most of the multiferroic materials belonged to either the perovskite (distorted perovskite) family or the hexagonal family or boracites or fluorites [1]. The key features of BFO such as antiferromagnetic ordering, spontaneous polarization and antiferrodistortion are specific to the distorted rhombohedral structure [2][3]. The effect of these properties individually or their coupling aids bismuth ferrite in potential application in many fields [4]. Perovskite bismuth ferrite ($BiFeO_3$–BFO) belongs to the class of single phase multiferroic material which has a rhombohedrally distorted cell with polar R3c space group. It was previously established that the stable phase of bismuth ferrite (BFO).

Bismuth ferrite ($BiFeO_3$ is an inorganic chemical compound with perovskite structure and one of the most promising multiferroic materials. The room-temperature phase of $BiFeO_3$ is classed as rhombohedral belonging to the space group R3c and Bismuth ferrite its the ternary compound[5][6]. It is synthesized in bulk and thin film form and both its antiferromagnetic (G type ordering) Neel temperature (approximately 653 K) and ferroelectric Curie temperature are well above room temperature (approximately 1100K)[7]. Ferroelectric polarization occurs along the pseudocubic direction with a magnitude of 90–95 $\mu C/cm^2$.

Bismuth iron oxide ($BiFeO_3$) presents multiferroic properties at room temperature since it exhibits both G-type antiferromagnetic order with a long-periodicity spiral

(TN ≈367 ºC) and ferroelectricity (TC ≈827ºC). Consequently it has been considered as a promising multiferroic material for potential applications in which coupling between magnetic and electrical order are involved. The processing electrical/electromechanical properties, basic physics and device application(s) have been thoroughly summarised by Catalan and Scott [8] and Rojac et al.[9]

Bismuth ferrite is one of the most extensively investigated multiferroic magnetoelectric compounds in which 6s lone pair electrons of Bi are believed to be responsible for ferro-electricity while partially filled d orbital of Fe leads to magnetic ordering. $BiFeO_3$ has a rhombohedral structure R_3c ($\alpha = \beta = \gamma = 59.4°$, a = b = c = 5.63 Å) at room temperature.

The ferroelectric polarization of bismuth ferrite aligns diagonals of pervoskite unit cell ([111]pseudocubic/[001]hexagonal). The ferroelectricity in bismuth oxide is less due to leakage current (oxygen vacancies). The local short-range magnetic ordering of $BiFeO_3$ is G-type antiferromagnetic whereas each Fe3+ spin is antiparallel to adjacent Fe3+ spins. The spins are in fact not perfectly antiparallel as there is a weak canting moment caused by the local magnetic coupling to the polarization. field.

$BiFeO_3$ is the only material that is both magnetic and a strong ferroelectric at room temperature, various BFO-based nanomaterials in different forms were prepared including BFO ceramics, thin films and nano-structures.

1.2 Statement of the problem

The study will be on the structural, electronic properties of $BiFeO_3$; which belongs to many body problem. **Many body problems** are complicated and challenging to solve. Because of this the state of motion cannot be solved analytically for systems in which three or more masses are interacting.

To solve this many body problems the density functional theory is preferred as an accurate and reliable tool. The basic purpose of DFT is that any property of the interacting systems can be viewed as a functional of the ground state density n_o(r).

However studying the structural, electronic properties of $BiFeO_3$ is very crucial to wider its application in future technologies. So it is aimed to investigate the structural, electronic properties of $BiFeO_3$ using DFT with the help of Quantum ESPRESSO

package. [10]

1.3 Research Questions

- What is the total minimum energy of Bismuth Ferrite ($BiFeO_3$) per cell with respect to cut-off energy?
- What is the total minimum energy of Bismuth Ferrite ($BiFeO_3$) per cell with respect to K-points sampling?
- What is the theoretical lattice constant of Bismuth Ferrite ($BiFeO_3$)?
- What is band structure of Bismuth Ferrite ($BiFeO_3$)?
- What is density of state of Bismuth Ferrite ($BiFeO_3$)?
- What is partial density of state of Bismuth Ferrite ($BiFeO_3$)?

1.4 Objectives of the study

1.4.1 General objective

The main aim of this study was to calculate the electronic and structural properties of Bismuth Ferrite ($BiFeO_3$) using density functional theory.

1.4.2 Specific objective

- To calculate the total minimum energy of Bismuth Ferrite ($BiFeO_3$) per cell with respect to cut-off energy.
- To calculate the total minimum energy of Bismuth Ferrite ($BiFeO_3$) per cell with respect to K-points sampling.
- To calculate the lattice constant of Bismuth Ferrite ($BiFeO_3$).
- To determine band structure of Bismuth Ferrite ($BiFeO_3$).
- To determine the total density of state of Bismuth Ferrite ($BiFeO_3$).
- To determine the partial density of state of Bismuth Ferrite ($BiFeO_3$).

1.5 Significance of the study

The significance of this study will help us to understand the structure and electronic properties of Bismuth Ferrite ($BiFeO_3$) using quantum espresso package. Moreover it helps to understand the electrical property of three dimensional BiFeO3. It also helps to compare the experimental results with respect to our calculation and understanding the structural, electronic properties of many electron system (BiFeO3) helps to know about the system in detail and to differentiate one material to other depending on their structure and electronic properties. Moreover it helps to develope computational skills for solving many body problems.

1.6 Scope of the study

The scope of this study is the calculations of electronic and structural properties of rhombohedral structure of $BiFeO_3$. However the total minimum energy and the lattice constants of $BiFeO_3$ were calculated with respect to cut-off energy and k-point samplings, while the band gap and density of states of $BiFeO_3$ were calculated based on density functional theory (DFT).

2

Review of Related Literature

2.1 General properties of perovskite Bismuth Ferrite $BiFeO_3$

$BiFeO_3$ or BFO is a material that drags a lot of attention in nowadays research due to its antiferromagnetic and ferroelectric properties which are shown at room temperature. It is commonly synthesized through sintering stoichiometric mixtures of Bi_2O_3 and Fe_2O_3 . Bismuth ferrite [$BiFeO_3$ (BFO)] is a conventional ABO_3-structured perovskite material with A and B sites occupied by Bi and Fe, respectively. It is the only multiferroic (ferroelectricity and ferromagnetism phenomena) system that can exhibit both the "ferro" orderings at room temperature.[13] [16]

Multiferroics belong to unique class of functional materials that show two or more 'ferroic' orders such as Ferroelectricity, Ferromagnetism and Ferroelasticity etc, at the same time.[12] Moreover coupling between magnetism and ferroelectricity in them could be used to induce electrical polarization by the magnetic field and vice versa. From the last few years a number of compounds such as $YMnO_3$, $BiMnO_3$, $BiFeO_3$ (BFO) etc. have been mentioned as the candidates belonging to the multiferroic type. Among them BFO attracts the most attention as a multiferroic material because it has simultaneously ferroelectric and antiferromagnetic properties even at room temperature.

$BiFeO_3$ is unique multiferroic material with multiple characteristics, the presence of high ferroelectric Curie temperature (Tc = 1103 K $\approx$ 830 ^{o}C and anti-ferromagnetic Neel temp (TN = 643 K $\approx$ 367 ^{o}C) makes it an ideal material for multifunctional devices. The electronic polarization of BFO is due to free electron pair in s-p hybrid orbital of Bi^{3+} ion while the magnetization arises from unpaired electrons in d orbital of Fe^{3+} ions [13]. BFO shows a G-type antiferromagnetic order which is Modulated to

a spiral spin structure whose modulation vector has a long period of $\lambda = 64$ nm [14], by reducing the crystallite and particle size by distorting crystal structure by introducing restriction in the thin films or by cationic substitution the AF-order of BFO can be changed thus leading to a ferromagnetic response. Also the antiferromagnetic order can be effectively modified by substitution at Fe^{3+} or Bi^{3+} sites. Additionally this substitution also promotes the asymmetry in crystal structure improving the electric polarization [15][16].

Multiferroics are an interesting domain of ceramic materials and has simultaneously attracted the interests of the researchers due to coexistence of two or more properties such as ferro or antiferromagnetism, ferroelectricity and ferroelasticity which offers a broad range of applications in photovoltaics, optics and electronic technology. One of its kind Bismuth Ferrite (BFO) or $BiFeO_3$ possesses the coexistence of properties such as ferroelectricity and antiferromagnetism at room temperature.

Bismuth ferrite as a material is an integral and the most important part of the multiferroics system. This review aims to compile the discussions related to the development of Bismuth ferrite based multiferroic ceramic materials which include the study of crystal structure properties and the role in synthesis of novel devices and implications in many other novel applications such as water treatment, energy generation, photovoltaics, piezoelectrics, high and ultra-high frequency range devices and so on.[16]

2.2 Crystal Structure of perovskite Bismuth Ferrite ($BiFeO_3$)

The perovskite $BiFeO_3$ (BFO) was first produced in the late 1950s, BFO has long been known to be in its bulk form an antiferromagnetic, ferroelectric multiferroic with an antiferromagnetic Néel temperature of TN = 643 K and a ferroelectric Curie temperature of TC = 1103 K.

We note that $BiFeO_3$ adopts the perovskite (Fig:2.1) and not the ferrite structure despite its nomenclature. Structure of Perovskite bismuth ferrite (BFO) exhibits a wide direct band gap of ($\sim$2.2 eV) with large visible light absorption up to 750 nm.

Bismuth ferrite oxide is one of the important single phase perovskite material its crystal structure possesses a rhombohedral distorted perovskite structure with R3c space

group at room temperature as shown in Fig:2.1 Furthermore bismuth ferrite material has a unique high ferroelectric Curie temperature (TC = 1103 K ≈ 830 °C) and antiferromagnetic Neel temperature (TN= 643 K ≈ 367 °C) which makes it suitable for high temperature applications[21]. Bulk bismuth ferrite can be described as a

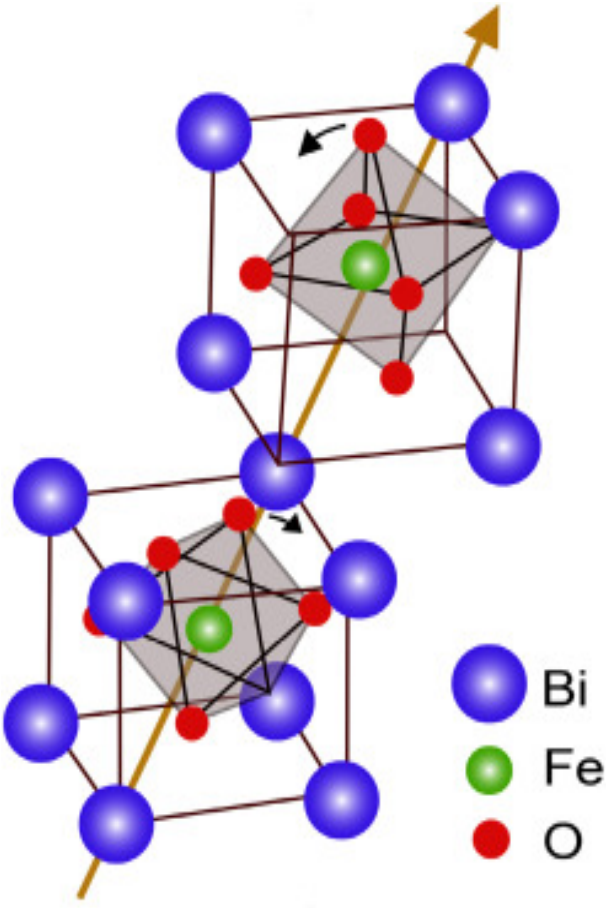

Figure 2.1: Crystal structure of perovskite $BiFeO_3$.

rhombohedrally distorted ferroelectric perovskite with the space group R3c (Fig:2.1). The lattice parameters of the rhombohedral unit cell are a = 5.59 Å and α = 60.68°. In such a distorted structure the R3c symmetry permits the development of spontaneous polarization(P_s) along the pseudocubic [111] direction.

The ground state of $BiFeO_3$ in room temperature has a rhombohedral symmetry and R3c space group. The R3c primitive unit cell is derived from the cubic perovskite by rotating the two neighbouring FeO_6 octahedra about the [111] axis in the opposite ways and displacing ions along [111] axis.

The ideal perovskite lattice has a Pm3m space group, the rotation of FeO_6 alone reduces the symmetry from Pm3m to centrosymmetric R3c space group while the displacement along [111] reduces the symmetry from Pm3m to rhombohedral R3m. The combination of these two deformations lowers the symmetry to R3c and makes $BiFeO_3$ polarized and highly distorted.[21]

2.3 Chemical properties of perovskite Bismuth Ferrite ($BiFeO_3$)

The chemical properties of perovskite chemical properties of Bismuth Ferrite are:

- It has a molecular weight of 312.82 g/mol.
- It has a crystalline solid appearance with a perovskite structure.
- It has a melting point 1255 ^{o}C.
- It has a density of 8.22 g/cm^3.
- It has a band gap of about 2.2 eV.
- It has a ferroelectric polarization of 90-95 μ C/m^2 along the pseudocubic direction.
- It has a G-type antiferromagnetic ordering with a Neel temperature of 653 K.
- It has a ferroelectric Curie temperature of 1100 K.
- It has a Bi and Fe valence state of 3+ in a 3:3 perovskite ratio[8][22].

2.4 Physical properties of perovskite Bismuth Ferrite ($BiFeO_3$)

Some of the physical properties of perovskite Bismuth Ferrite are:

- It has a rhombohedrally distored perovskite structure in its bulk form where the Bi^{+3} and Fe^{+3} cation are displaced from their centrosymmetric positions along the (111) axise.
- It has a high ferroelectric curie temperature of 1100 K and a low antiferromagnetic Neel temperature of 640 K.

- It has a modulated spin spiral structure of periodicity 62 nm.
- It has a high dielectric constant of 1000 at room temperature.
- It has a large remanent polarization of about 60 $\mu C/m^2$ at room temperature.
- It has low coercive field of 50 kV/cm at room temperature.
- It has a high magnetoelectric coupling coefficient of about 10^{-7} S/m at room temperature.
- It has a low electrical conductivity of about 10^{-9} S/cm at room temperature.
- It has a high optical band gap of 2.7 eV at room temperature electric[3][8]

2.5 Electronics properties of pervoskite Bismuth Ferrite ($BiFeO_3$)

The electronics of pervoskite bismunth ferrite are determined by the interaction between the electron and the lattice vibrations (phonons) in the material the electrons can be affected by the electric polarization and the magnetic ordering of the material which can change the electronic band structure, the conductivity and the optical properties of the material[8].
Some of the factors that influence the electronics of pervoskite Bismuth Ferrite are listed below:-

- The A-site doping which can modify the valence state of the bismuth and iron ions and create oxygen vacancies. This can affect the ferroelectric polarization the magnetic ordering and the electrical conductivity of the material.
- The B-site doping which can introduce different transition metal ions the A-site doping such as manganese, cobalt and nickel and create mixed valence states. This can affect the magnetic ordering the magnetoelectric coupling and the optical properties of the material.
- The heterojunction formation which can create a contact between perovskite bismuth ferrite and another material such as graphene, titanium dioxide or silver. This can affect the charge transfer the interface states and the photocatalystic perfomance of the material.

2.6 Application of pervoskite Bismuth Ferrite ($BiFeO_3$)

There are so many applications of Bismuth Ferrite(BFO) in our daily life as TV satellite communication and in audio video recordings. An important application of BFO is $Bi_2Fe_4O_9$. It is used as semiconductor gas sensor and as a good catalyst.
Due to the advantages of excellent performance BFO materials display great potentials for designing and developing a wide variety of devices with novel functions. In this we will focus on the application fields of electronics, spintronics and photonics devices.

2.6.1 Electronics devices

BFO-based nanomaterials have both ferroelectricity and ferromagnetism at room temperature showing great potential for applications in high-density ferroelectric devices such as nonvolatile memories. However to obtain the fast high-density nonvolatile data storage and logic devices is dependent on a robust reversibly switchable with low operation speed stability and persistence. Thus a variety of attempts were made to tune the ferroelectric resistive switching in BFO-based nanomaterials. Using an atomically tetragonal BFO ultra thin film. Observed a stable ferroelectric polarization and its switching behavior.[16][17]

2.6.2 Spintronic devices

The property of magnetoelectric coupling under the room temperature results in that it is possible to control the magnetic behaviors by an electric field for BFO-based nanomaterials. As a result BFO-based material becomes a candidate for applications in spintronic devices.[18] Proposed a giant magnetoresistive device based on BFO by spin valve exchange to investigate the prospect of BFO-based nanomaterials in electrically written spintronic devices.
The device structure was Sulfated tin oxide(STO) strontium oxide(SrO) Bismuth Ferrite-Magnanes(BFO-Mn) Bismuth ferrite(BFO) Cobalt Iron Boron(CoFeB) Copper(Cu) and Cobalt(Co) where a giant magnetoresistance signal was tested. Moreover the exchange bias was regulated by the applied voltages.
However poor stability of the Bismuth ferrite(BFO) Cobalt Iron Boron(CoFeB) inter-

faces seriously hindered the increase of giant magnetoresistance signal. Explored the thermal stability of the BFO/CoFeB interface and revealed the physical mechanism. It demonstrated that the difference of oxygen vacancies induced by BFO polarization direction was the key that influenced the thermal stability.[18][20]

2.6.3 Optics devices

Driven by growing demand for clean and renewable energy ferroelectric photovoltaic nanomaterials which can convert solar energy into electricity have attracted more and more attention. As compared with the traditional ferroelectric nanomaterials BFO-based nanomaterials present unique performances such as the narrow band-gap, better carrier transport and light absorption characteristics. Thus it is of significance to develop ferroelectric photovoltaic devices based on BFO nanomaterials[19] [20], have made outstanding works in the photovoltaic application fields based on BFO nanomaterials.

2.7 Density Functional Theory (DFT)

Density functional theory (DFT) is a successful theory to calculate the electronic structure of atoms, molecules, and solids. Its goal is the quantitative understanding of material properties from the fundamental laws of quantum mechanics. Density functional theory (DFT) is one of the most widely used methods for ab initio calculations of the structure of atoms, molecules, crystals, surfaces, and their interactions. Density functional theory is a theory of correlated many-body systems. The fundamental principle of density functional theory is that any property of a system of many interacting particles can be viewed as a functional of the ground state density $\mathbf{n_0}(\mathbf{r})$; that is, one scalar function of position $\mathbf{n_0}(\mathbf{r})$, in principle, determines all the information in the many-body wave functions for the ground state and all excited states[25][43]. Quantum condensed matter physics deals with the interplay of quantum mechanics with the presence of a very large number of coupled degrees of freedom $\sim 10^{24}$. This interplay leads to a rich plethora of emerging properties that find their way into our daily life: metals, semi-metals, insulators, superconductors etc. the Following the complexity of the many-electron problem, there have been a number of attempts to simplify the problem and avoid a direct solution of the Schrödinger

equation [23]. Such attempts are Born-Openheimer approximation, Hartree-Fock theory, Hohenberg-kohn theory, Thomas-Fermi theory, the Kohn-Sham theory, the modern DFT, exchange correlation functionals and some other approximations are discussed in detail.

2.8 Many electron system

The Hamiltonian for a Quantum system with M nuclei at positions R_i and N electrons at positions r_i [25] is:

$$\hat{\boldsymbol{H}} = \hat{\boldsymbol{T}} + \hat{\boldsymbol{V}} \tag{2.1}$$

$$\hat{\boldsymbol{T}} = -\sum_{i=1}^{\boldsymbol{M}} \frac{\hbar^2 \boldsymbol{\nabla}^2_{\boldsymbol{R_i}}}{\boldsymbol{2M_i}} - \sum_{i=1}^{\boldsymbol{N}} \frac{\hbar^2 \boldsymbol{\nabla}^2_{\boldsymbol{r_i}}}{\boldsymbol{2m}} \tag{2.2}$$

For the potential energy term, we have the Coulomb repulsion between electron-electron, electron nuclei-nuclei and electron nuclei:

$$\hat{\boldsymbol{V}} = \frac{\boldsymbol{1}}{\boldsymbol{2}} \sum_{i,j<N}^{\boldsymbol{N}} \frac{\boldsymbol{e^2}}{|\boldsymbol{r_i} - \boldsymbol{r_j}|} + \frac{\boldsymbol{1}}{\boldsymbol{2}} \sum_{i,j<M}^{\boldsymbol{M}} \frac{\boldsymbol{Z_i Z_j e^2}}{|\boldsymbol{R_i} - \boldsymbol{R_j}|} - \sum_{i=1}^{\boldsymbol{M}} \sum_{j=1}^{\boldsymbol{N}} \frac{\boldsymbol{Z_i e^2}}{|\boldsymbol{R_i} - \boldsymbol{R_j}|} \tag{2.3}$$

From 2.2 and 2.3, we have the total Hamiltonian

$$\begin{aligned} \hat{\boldsymbol{H}} = -\sum_{i=1}^{\boldsymbol{M}} \frac{\hbar^2 \boldsymbol{\nabla^2 R_i}}{\boldsymbol{2M_i}} + \frac{\boldsymbol{1}}{\boldsymbol{2}} \sum_{i \neq j<M}^{\boldsymbol{M}} \frac{\boldsymbol{Z_i Z_j e^2}}{|\boldsymbol{R_i} - \boldsymbol{R_j}|} - \sum_{i=1}^{\boldsymbol{N}} \frac{\hbar^2 \boldsymbol{\nabla^2 r_i}}{\boldsymbol{2m}} \\ - \sum_{i=1}^{\boldsymbol{M}} \sum_{j=1}^{\boldsymbol{N}} \frac{\boldsymbol{Z_i e^2}}{|\boldsymbol{R_i} - \boldsymbol{R_j}|} + \frac{\boldsymbol{1}}{\boldsymbol{2}} \sum_{i \neq j<N}^{\boldsymbol{N}} \frac{\boldsymbol{e^2}}{|\boldsymbol{r_i} - \boldsymbol{r_j}|} \end{aligned} \tag{2.4}$$

$$\hat{\boldsymbol{H}} \boldsymbol{\Psi}(\boldsymbol{r_i}, \boldsymbol{R_i}) = \boldsymbol{E} \boldsymbol{\Psi}(\boldsymbol{r_i}, \boldsymbol{R_i}) \tag{2.5}$$

Where Ψ the many-body wave function and E is the total energy of the system in the quantum state specified by the many-body wave function Ψ. The kinetic energy of N electrons and M nuclei in such a quantum system is given by: From 2.4 and 2.5 , we have

$$\begin{aligned} \Big[-\sum_{i=1}^{\boldsymbol{M}} \frac{\hbar^2 \boldsymbol{\nabla^2}}{\boldsymbol{2M_i}} + \sum_{i \neq j<M}^{\boldsymbol{M}} \frac{\boldsymbol{Z_i Z_j e^2}}{\boldsymbol{2}|\boldsymbol{R_i} - \boldsymbol{R_j}|} - \sum_{i=1}^{\boldsymbol{N}} \frac{\hbar^2 \boldsymbol{\nabla^2}}{\boldsymbol{2m}} - \sum_{i=1}^{\boldsymbol{M}} \sum_{j=1}^{\boldsymbol{N}} \frac{\boldsymbol{Z_i e^2}}{|\boldsymbol{R_i} - \boldsymbol{R_j}|} \\ + \sum_{i \neq j<N}^{\boldsymbol{N}} \frac{\boldsymbol{e^2}}{\boldsymbol{2}|\boldsymbol{r_i} - \boldsymbol{r_j}|} \Big] \boldsymbol{\Psi}(\boldsymbol{r}, \boldsymbol{R}) = \boldsymbol{E} \boldsymbol{\Psi}(\boldsymbol{r}, \boldsymbol{R}) \end{aligned} \tag{2.6}$$

Or in more compact notation,

$$\hat{\boldsymbol{H}} = \hat{\boldsymbol{T}}_{\boldsymbol{N}} + \hat{\boldsymbol{V}}_{\boldsymbol{NN}} + \hat{\boldsymbol{T}}_{\boldsymbol{e}} + \hat{\boldsymbol{V}}_{\boldsymbol{Ne}} + \hat{\boldsymbol{V}}_{\boldsymbol{ee}} \tag{2.7}$$

where M_i is mass of i^{th} nucleus, m is mass of electron, $\hbar$ is the reduced Planck constant, Z_i is the charge of i^{th} nucleus, e is the charge of electron In (2.4) the first and third terms are the kinetic energies of nuclei and electron respectively. And the 2^{nd}, 4^{th} and 5^{th} terms are the ion-ion, ion-electron and electron-electron interactions respectively.

For N particles in classical system the momenta and position are known exactly. But in Quantum system, consider two Bi atoms which have $83 \times 2 = 164$ electrons. One electron has three spatial coordinates. So,164 electrons will have $164 \times 3 = 492$ spatial coordinates. In addition Bi atoms have $164 \times 2 = 328$ spin coordinates and therefore, Bi atoms have total of $492 + 328 = 820$ coordinates which makes 2.6 complicated and difficult to interpret. The trouble is that the solution of the above equation for all but the simplest systems (e.g. small molecules) is very challenging, and in most cases it is still practically impossible. As a result, today there exists a spectacular hierarchy of approximations to equation 2.4 or 2.6, which allow us to study materials at the atomistic level with varying degrees of sophistication and accuracy[26].

For approximately solving many electron problems; different theories, appropriate approximations and exchange correlations are important.

2.9 Electron Density

The electron density n(r) is defined as the number of electrons per volume at the point r in space. The integral of the electron density gives the total number of electrons,

$$\int \boldsymbol{n}(\boldsymbol{r})\boldsymbol{dr} = \boldsymbol{N} \tag{2.8}$$

The Born-Oppenheimer approximation separates the above many body wave function 2.5 in to independent states for nuclei ψ_n and electrons ψ_e, with energies E_n and E_e.

$$\boldsymbol{\Psi} = \boldsymbol{\psi_n}\boldsymbol{\psi_e} \tag{2.9}$$

The relation between n(r) and the many-electron wave-function ψ_e is [27]

$$n(r) = N \int \int ... \int |\psi_e(r\sigma_1, x_2, ...x_N)|^2 d\sigma_1 dx_2 ... dx_N \tag{2.10}$$

2.10 Born-Oppenheimer Approximation

By Born-Oppenheimer approximation the nuclear kinetic energy is zero (nuclei much slower than the electrons) and their potential energy is merely a constant (nuclear positions are fixed)[28, 29]. Then equation 2.7 becomes

$$\hat{H} = \hat{T}_e + \hat{V}_{Ne} + \hat{V}_{ee} \tag{2.11}$$

2.11 Hartree - Fock theory

Hartree-Fock theory is fundamental to much of electronic structure theory. It is the basis of molecular orbital (MO) theory, which posits that each electron's motion can be described by a single-particle function (orbital) which does not depend explicitly on the instantaneous motions of the other electrons. Hartree-Fock theory was developed to solve the electronic Schrödinger equation that results from the time-independent Schrödinger equation after invoking the Born-Oppenheimer approximation. In atomic units, and with r denoting electronic and R denoting nuclear degrees of freedom, the electronic Schrödinger equation[29].

$$\Big[-\frac{1}{2}\sum_i \nabla_i^2 - \sum_{A,i} \frac{Z_A}{r_{A_i}} + \sum_{A>B} \frac{Z_A Z_B}{R_{AB}} + \sum_{i>J} \frac{1}{r_{ij}} \Big] \Psi(\boldsymbol{r};\boldsymbol{R}) = \mathrm{E}\Psi(\boldsymbol{r};\boldsymbol{R}) \tag{2.12}$$

or, in more compact notation,

$$\Big[\hat{T}_e(\boldsymbol{r}) + \hat{V}_{Ne}(\boldsymbol{r};\boldsymbol{R}) + \hat{V}_{NN}(\boldsymbol{R}) + \hat{V}_{ee}(\boldsymbol{r})\Big] \Psi(r;R) = \mathrm{E}\Psi(r;R) \tag{2.13}$$

Therefore, the total energy of interacting Hamiltonian

$$H = -\frac{1}{2}\sum_i \nabla_i^2 + \hat{V}_{int}(ee) + E_{II} + \hat{V}_{ext} \tag{2.14}$$

2.12 Thomas Fermi Theory

The key idea in Thomas Fermi theory and its generalizations is the replacement of complicated terms in the kinetic energy and electron–electron repulsion energy contributions to the total energy by relatively simple functional of the electron density.

The Thomas Fermi theory is the simple example of a DFT. It emerges when we ignore the exchange energy and make the simplest possible approximation for the kinetic energy. For a solely varying density function the kinetic energy density will only depend on the number of density at the same position. Taking the specific function from the Fermi gas, we arrive at the kinetic energy functional. In Thomas-Fermi method the kinetic energy of system of electrons is approximated as an explicit functional of the density considered as non-interacting electron gas. If E[n] is energy per-particle of homogeneous electron gas of density[n] and n(r) local density given total energy [30, 31, 32].

$$\boldsymbol{E[n] = \int E(n)n(r)dn} \tag{2.15}$$

In electrostatic screening in region where there is no electrostatic contribution to chemical potential.

$$\boldsymbol{E_F = \frac{\hbar^2}{2m}(3\pi^2)^{\frac{3}{2}}n(r)^{\frac{2}{3}}} \tag{2.16}$$

$$\boldsymbol{E[n] = \frac{1}{2}(3\pi^2)^{\frac{3}{2}}n(r)^{\frac{2}{3}}}$$

$$\boldsymbol{T[n(r)] = \int E[n]n(r)dr = \frac{1}{2}(3\pi^2)^{\frac{3}{2}}(\frac{3}{5})\int (n)^{\frac{5}{3}}(r)dr}$$

$$\boldsymbol{T[n(r)] = \frac{3}{10}(3\pi^2)^{\frac{3}{2}}\int (n)^{\frac{5}{3}}(r)dr} \tag{2.17}$$

Coulomb interaction

$$\boldsymbol{E_c = \frac{1}{2}\int \frac{n(r)n(r^{'})}{|r-r'|}drdr^{'}} \tag{2.18}$$

$$\boldsymbol{E_{ext} = \int n(r)V_{ext}(r)dr} \tag{2.19}$$

$$\boldsymbol{E[n(r)] = T[n] + E_c[n] + E_{ext}[n]} \tag{2.20}$$

In Thomas Fermi theory exchange energy is included. For homogeneous electron gas

$$\boldsymbol{E_{xc}[n(r)] = -\frac{3}{4}(\frac{3}{\pi})^{\frac{1}{3}}\int n^{\frac{4}{3}}(r)dr}$$

Total energy

$$E_{TF}[n(r)] = E[n(r)] + E_{xc}[n(r)] \tag{2.21}$$

And the sum of the KE and potential energy terms will give us the total energy within the Thomas Fermi approximations[49]

$$\begin{aligned} E\left[n\left(r\right)\right] = & \int \frac{3}{10}\frac{\left(3\pi^2\right)^{\frac{2}{3}}}{m} n\left(r\right)^{\frac{5}{3}} d^3 + \frac{e^2}{2}\int \frac{n\left(\overrightarrow{r}\right) n\left(\overrightarrow{r}\prime\right)}{|\overrightarrow{r} - \overrightarrow{r}\prime|} d^3\overrightarrow{r}\prime d^3\overrightarrow{r} \\ & + \int n\left(r\right) V_N\left(r\right) d^3 r \end{aligned} \tag{2.22}$$

Where the first term is kinetic energy of the electrons, the second term is the potential energy of the electrons due to their mutual electric repulsion and the third term is the potential energy of an atom's electrons, due to the electric attraction of positively charged nucleus. Note that the expression only depends on density n(r). Unfortunately, this theory has limited validity due to its poor approximation of kinetic energy functional

2.13 Hohenberg-Kohn Theorem

The foundation of the DFT method is the Hohenberg-kohn theorem, which states that for each given electronic density $\rho(r)$, there is one and only one corresponding potential. The approach of Hohenberg and Kohn is to formulate density functional theory as an exact theory of many-body systems. All properties of the many body system are determined by ground state density. The H-K theorem implies that the ground-state for any system can be determined by varying the charge density until the global minimum in the energy functional is found[49].

Theorem 1: The ground state energy of many body system is a unique functional of the ground electron density. In principle all properties of the ground state can be expressed as functional of the ground state spin density matrix ρ_o.

$$E_0 = E[n_0(r)] \tag{2.23}$$

The ground state wave function ψ can also be determined by the density function theory) minimizing the energy functional Using $\psi_o\rho_o$ one can determine all properties by calculating;

$$\langle\widehat{o}\rangle\left[\rho_o\right] = \langle\psi_o\left[\rho_o\right]|\widehat{o}|\psi_o\left[\rho_o\right]\rangle \tag{2.24}$$

Where $\widehat{o}$ is an arbitrary operator.

Theorem 2: A universal functional for the energy $\boldsymbol{E}[\boldsymbol{n}]$ in terms of the density n(r) can be defined, valid for any external potential $\boldsymbol{V_{ext}}(\boldsymbol{r})$. For any particular $\boldsymbol{V_{ext}}(\boldsymbol{r})$, the exact ground state energy of the system is the global minimum value of this functional, and the density that minimize the functional is the exact ground state density $\boldsymbol{n_o}$ (r)[34]. The total energy can be written as,

$$\boldsymbol{E}\left[\boldsymbol{n}\right] = \boldsymbol{T}\left[\boldsymbol{n}\right] + \boldsymbol{V_{ne}}\left[\boldsymbol{n}\right] + \boldsymbol{V_{ee}}\left[\boldsymbol{n}\right] = \boldsymbol{F_{HK}}\left[\boldsymbol{n}\right] + \boldsymbol{V_{N_e}}\left[\boldsymbol{n}\right] \tag{2.25}$$

Where ;$F_{HK}\left[n\right] = T\left[n\right] + V_{ee}\left[n\right]$ which is universal functional.

2.14 Kohn-Sham Approach/ theory

In 1965 Kohn and Sham took the total energy in the independent electron approximation as the combination of kinetic and Coulomb energy of independent electrons and the exchange and correlation energy that accounts for all the difference. The Hohenberg and Kohn theorems facilitate the treatment of quantum systems by stating, that the electron density of the ground state completely describes a system. Kohn and Sham (KS) proposed to put wave mechanics in to the kinetic energy functional, but retain the density variable n(r) elsewhere. Their theory was tightly linked to Hartree-Fock slater approximation of many body fermions theory[34, 35]. The weakest part of the Thomas Fermi theory was the treatment of the kinetic energy functional in this theory. Kohn-sham considered the exchange and correlation energies and supposed to calculate the exact kinetic energy of a non interacting reference system with the same density as the real interacting system.

$$\boldsymbol{E}[\boldsymbol{n}] = \boldsymbol{T_s}[\boldsymbol{n}] + \boldsymbol{E_H}[\boldsymbol{n}] + \boldsymbol{E_{ext}}[\boldsymbol{n}] + \boldsymbol{E_{xc}}[\boldsymbol{n}] \tag{2.26}$$

The functional E_H[n] is the classical(Hartree) interaction energy between the N particles with density n, including their self-interaction energy. E_H[n] is usually referred to as Hartree term.

$$\boldsymbol{E_H}[\boldsymbol{n}] = \frac{\boldsymbol{1}}{\boldsymbol{2}} \int \boldsymbol{d^3 r} \int \boldsymbol{d^3}(\boldsymbol{r'})\boldsymbol{n}(\boldsymbol{r})\boldsymbol{w}(\boldsymbol{r},\boldsymbol{r'})\boldsymbol{n}(\boldsymbol{r'}) \tag{2.27}$$

E_{ext}[n] characterizes the coupling between the particles and the external potential,

$$\boldsymbol{E_{ext}}[\boldsymbol{n}] = \int \boldsymbol{d^3 r} \boldsymbol{v_{ext}}(\boldsymbol{r})\boldsymbol{n}(\boldsymbol{r}) \tag{2.28}$$

$$E_{ext}[n] = \int d^3 r v_{ext}(r) n(r) \tag{2.29}$$

The kinetic energy functional T_s[n] of non-interacting particles for any ground state density n resulting from a Hamiltonian can be expressed in terms of the single-particle orbitals ϕ_i

$$aT_s[n] = \sum_i \Theta_i \sum_{\sigma=\uparrow,\downarrow} \int d^3 r \phi_{i^*}(\overrightarrow{r}\sigma) \frac{(-i\hbar\overrightarrow{\nabla})^2}{2m} \phi_i(\overrightarrow{r}\sigma) \tag{2.30}$$

Finally, the exchange-correlation(xc) energy functional $E_{xc}[n]$ is defined by 2.26. It absorbs all the complicated many-body effects not contained in T_s , E_H and E_{ext}. $E_{xc}[n]$ is a density functional as, on the one hand, E[n] is a density functional by virtue of the HK theorem for interacting particles and, on the other hand, T_s is a density functional by virtue of the HK theorem for non-interacting particles, while E_H and E_{ext} are explicit density functional.

2.15 Exchange- Correlation Energy

The exchange-correlation energy E_{xc} of a many- electron system is the quantity of DFT. In context of Kohn-Sham theory, E_{xc} is defined as a functional of the electron density n. In K-S expression the total electronic energy $E[n]$ is[27];

$$E[n] = T_s[n] + V_{Ne}[n] + W_H[n] + E_{xc} \tag{2.31}$$

Where; T_s - is the kinetic energy of a non-interacting particle system with density n, V_{Ne}[n] is the energy of electron-nuclear attraction, W_H is the coulomb or Hartree energy and E_{xc} is the exchange-correlation energy. An accurate values of the exchange and correlation energies obtained for chemically interacting systems are essential for analysis of the effect of electron correlation with the Kohn-sham theory and in order to test and calibrate various DFT approximation (Local Density Approximation(LDA) and Generalized Gradient Approximation(GGA)).[33].

2.15.1 Local Density Approximation (LDA)

The first family of exchange correlation functional is the LDA functional [36]. The idea of this functional is the first look at the case of a homogenous electron gas. In such a

system, one considers the electron moving in uniform external potential. In DFT, the electron density rather than the wave function is the basic variable.

$$E_{xc}^{LDA}[n] = \int n(r) E_{xc}[n(r) d\widehat{r}] \tag{2.32}$$

In LDA, there is no known formula to calculate the total energy of many electrons moving in an external potential using the density. Hohnberg and Kohn proved that there exist a universal functional of the density called,$G[n]$ such that:

$$E[n(r)] = \int v(r) n d^3r + \frac{1}{2} \int \frac{n(r)n(r')}{|r-r|} d^3r d^3r' + G[n] \tag{2.33}$$

Where the first term on the right hand side is the energy due to external potential while the second term is the classical coulomb energy of the electron system. The main deficiency of the LDA was the strong over binding with bond energies in error by about 1 eV. On the one hand this renders LDA useless for most applications in condensed matter physics. On other hand, the problem was hardly visible in solid state physics where bonds are rarely broken, rearranged so that the errors canceled.

2.15.2 Generalized Gradient Approximation (GGA)

This functional (GGA) depends on the local electron density as the spatial variation of the electron density that is represented by density gradient. The idea behind this functional was to improve the approximation of LDA by considering not only the electron density, but also the local gradient of that density [37, 38]. The GGA functional can be written as;

$$E_{xc}^{GGA}[n] = \int n(r) E_{xc}[n(r) \bigtriangledown_n] d\overrightarrow{r} \tag{2.34}$$

The $E_{xc}^{GGA}[n]$ is the exchange correlation energy per particle of an electron gas. The GGA gives better total energies. When a bond between two atoms is broken, the surface is increased. In GGA, this bond-breaking process is more favorable than in LDA and hence bond is weakened. Thus the GGA cures the over binding error of the LDA. These gradient corrections greatly improved the bond energies and made density functional theory useful also for chemists. The most widely distributed GGA functional is the Perdew Burke-Ernzerhof (PBE) functional.

2.16 Plane wave basis sets and Pseudo potentials

2.16.1 Plane wave basis set

In calculations of solid states or condensed matter, the DFT will be applied with plane wave basis sets. When dealing with a crystal which has atoms periodically arranged, the electrons are in a periodic potential U(r), where $\boldsymbol{U(r+R)=U(r)}$ and R is the Bravais lattice. As the Bloch theorem states below that, a discrete plane- wave basis sets are used to expand the electronic wave function at each K-points. In principle, an infinite plane wave basis sets is required to expand the electronic wave function. However, the coefficients $\boldsymbol{C_i, K+G}$ for the plane waves with small kinetic energy, $\boldsymbol{\frac{\hbar}{2m}|K+G|^2}$ are typically more important than those with large kinetic energy. Thus, plane-wave basis sets can be truncated to include only plane wave that have kinetic energy less than some particular cut-off energy. [39]

2.16.2 Pseudo-potential

Pseudo potentials have been introduced to avoid describing the core elements explicitly and to avoid the rapid oscillation of the wave function near the nucleus, which normally require either complicated or large base sets. Due to this, the fundamental idea of pseudo potential is the replacement of one problem with another. Its primary application in electronic structure is to replace the strong coulomb potential of the nucleus and the effects of tightly bound core electrons by an effective ionic potential acting on the valence electron [40]. The pseudo potential approximation is motivated by the fact that the behavior of valence electrons in the bonding region primarily determines the electronic structure and the structural properties of many materials. In a pseudo-potential formulation, the effect of the core electrons and that of nuclear potential are combined to form an effective ionic pseudo-potential. The pseudo potentials are commonly constructed, so that outside of a core region the valence pseudo wave functions match the corresponding states derived from all electron calculation, inside the region they are smooth functional. This formulation makes pseudo-potential calculations quite efficient, since the core orbital do not need to be recomputed. The relaxation correction takes in to account the relaxation

of the electron system up on the excitation of an electron. The orthogonalized plane waves ($\boldsymbol{OPW}$) is defined by

$$\psi_k^{OPW} = e^{ik.\overrightarrow{r}} + \sum_c b_c \psi_k^c \left(\overrightarrow{r}\right) \tag{2.35}$$

where $\psi_k\left(r\right)$ is the core wave function the sum is over all core levels with Bloch wave vector k, and we require that ϕ_k are orthogonal to every core level. The starting point for pseudo potential calculations and analysis is the application of nearly free electron (NFE) theory to find the valence levels (ϕ_k^v). The pseudo potential is the sum of the actual periodic potential and $\boldsymbol{V^R}$ Where;
$v^R = \Sigma_c \left(E_k^v - E_c\right)\left(\int dr \psi_K^{c^*} \phi\right) \psi_k^c$

$$H + V^R = -\frac{\hbar^2}{2m} + U + V^R \tag{2.36}$$

Where; $U + V^R = Vspendo$, U- is negative near ion cores while $\boldsymbol{V^R}$ is always positive. Moreover pseudo potentials have been introduced to avoid the rapid oscillations of the wave function near the nucleus, which normally require either complicated or large basis sets and to avoid describing the core electrons explicitly. Hamann, Schluter and Chiang showed in 1979 how pseudo-potentials can be constructed in such a way that their scattering properties are identical to that of an atom to first order in energy. These first principles pseudo potentials relieved the calculation from the restrictions of empirical parameters. Highly accurate calculations have become possible especially for semiconductors and simple metals. An approach by Zunger and Cohen towards first principles pseudo potentials precedes other approaches[42].

2.17 Periodic super cells

The vectors that decane the cell volume and the atom positions within the cell are collectively referred to as the super cell, and the definition of a super cell is the most basic input into a DFT calculation[43]. We would define the shape of the cell that is repeated periodically in space, the super cell, by lattice vector $\overrightarrow{a_1}$, $\overrightarrow{a_2}$, and $\overrightarrow{a_3}$. If we solve the Schrödinger equation for this periodic system, the solution must satisfy a fundamental property known as Bloch's theorem.

2.17.1 Bloch theorem

In condensed matter physics, Bloch's theorem states that solutions to the Schrödinger equation in a periodic potential take the form of a plane wave modulated by a periodic function. The theorem is named after the physicist Felix Bloch, who discovered the theorem in 1929. A Bloch function is the generalization of a plane wave for an electron in periodic potential.[28, 44]

$$\psi_k(r) = e^{iG.\vec{r}} U_k(r) \tag{2.37}$$

Where $U_k(\hat{r})$ is the periodic potential in space with the same periodicity as the supper cell. That is;

$$U_k(\hat{r}) = U_k\left(\vec{r} + n_1\vec{a_1} + n_2\vec{a_2} + n_3\vec{a_3}\right) \tag{2.38}$$

where for any integer $\vec{a_1}$, $\vec{a_2}$ and $\vec{a_3}$

2.17.2 Energy cut-off

Energy cut-offs limit the number of plane wave components. The minimum length scale depends on the elements in the system. The selection of cut-off energy also depends on the selection of pseudopotential for each atom. The size of the Hamiltonian matrix, N, is given by the number of reciprocal lattice vectors G. In the first-principles calculation, we do not usually compare N for different calculations but cut-off energy in units of atomic unit which is defined by

$$E_{cutoff} = \frac{\hbar^2}{2m} G_{max}^2 \tag{2.39}$$

where G_{max} is the largest reciprocal lattice vector.[40, 41]

2.17.3 K- Points

Our discussion of k-space would begin with Bloch's theorem, which tells us the solutions of the Schrödinger equations for a super cell that have the form

$$\psi_k(r) = e^{iG.\vec{r}} U_k(r) \tag{2.40}$$

where $U_k(r)$ is periodic in space with the same periodicity as the supper cell. It is now time to look at this part of the problem more carefully. The periodicity of $U_k(r)$

means that it can be expanded in terms of a special set of plane waves $e^{i(K+G).r}$.

$$U_k(r) = \Sigma C_{i'G} e^{i(K+G).r} \tag{2.41}$$

Where the summation is over all vectors defined by; $\overrightarrow{G} = n_1 \overrightarrow{b} + n_2 \overrightarrow{b} + n_3 \overrightarrow{b}$ With integer values n_i. The set of vectors defined by $\overrightarrow{G}$ in reciprocal space are defined. So that for any real space lattice vector, combining the two equations above give

$$\overline{\Psi}_k(r) = \Sigma_G C^{ik+Ge} \left(\left(i\overrightarrow{K} + \overrightarrow{G} \right) \overrightarrow{r} \right) \tag{2.42}$$

According to this expression, evaluating the solution at even a single point in k-space involves a summation over an infinite number of possible values of G. This does not use for practical calculations. Here are solutions with kinetic energy.

$$E = \frac{\hbar^2}{2m} |\overrightarrow{K} + \overrightarrow{G}|^2 \tag{2.43}$$

It is reasonable to expect that the solutions with lower energies are more physically important than solutions with very high energies. As a result, it is usual the infinite sum above to include only solutions with kinetic energies less than some value; The infinite sum then reduces to

$$\psi_k(r) = \Sigma_{|G+K|<G} CG + Ke^{\left[i\left(\overrightarrow{K}+\overrightarrow{G}\right)r \right]} \tag{2.44}$$

This expression includes slightly different numbers of terms for different values of k. The discussion above has introduced one more printer that must be defined whenever a DFT calculation is performed the cutoff energy (E_{cut}). The solution that is used most widely was developed by monk-horst pack in 1976. The symmetry of the cell may be used to reduce the number of k-points which are needed. Using these methods, one can obtain an accurate approximation for the electronic potential and the total energy of an insulators or semiconductor by calculating the electronic states at a very small number of k-points. The electronic potential and total energy are more difficult to calculate if the system is metallic because a dense set of k-points is required to define the Fermi surface precisely. The magnitude of any error in the total energy due to inadequacy of the k-points sampling can always be reduced by using a denser set of k-points. The computational cost of performing a very dense sampling of k-points can be significantly reduced by using the k-point total energy method [40, 45].

3

Materials and Computational Methodology

3.1 Materials

The main source of review literature from published articles, books, dissertations were carried out according to project title. Soft-wares(Fortran 90/95 computer program, QUANTUM ESPRESSO package), xcrysden software, Latex(TeXstudio) software and computer(64-bit) are additional instruments, which will be used to accomplish the project work.

3.2 Computational Methodology

Our study was based on Density Functional Theory (DFT) first-principles (ab-initio) calculations of structural and electronic properties of Bismuth Ferrite $BiFeO_3$. The calculation was performed computationally using Quantum Espresso which is an open-source package for research in electronics structure, simulation and optimization. The Quantum Espresso software package is an integrated suite of computer code for electronic structure calculations and materials modeling based on (DFT) and quantum espresso packages PWscf (Plane-Wave Self-Consistent Field) and CP (Car-Pirandello) for the calculation of electronics-structure properties with in density-functional theory using a plane-wave (PW) basis set and pseudo-potentials. In this study, the first principles calculations of the structural and electronic properties of $BiFeO_3$ was performed by using density functional theory(DFT). For ionic potentials, projector augmented wave (PAW) method was used. The generalized gradient approximation(GGA) of Perdew-Burke-Ernzerhof(PBE) formalism [47] was adopted for the exchange-correlation potential. It is important to choose the basis over which the Kohn Sham equation can be expanded. During the calcula-

tions, the cutoff energy was set to appropriate value and the Brillouin zone sampling by the Monkhorst-Pack k-mesh[45] was also sampled to a suitable size. For the ground state calculation, the computational parameters must be used exactly to solve for the Kohn-Sham eigenvalues. The optimized structure was then used to calculate the electronic properties, in particular the energy gap. The core electrons with strong coulombic effect were treated using the Troullier and Martins pseudo potentials [48]. The computation takes place in such a way that input file is given for the soft-ware (Quantum Espresso Package). The input file is composed of three mandatory name lists &CONTROL, &SYSTEM, &ELECTRONS, followed by three cards ATOMIC_SPECIES, ATOMIC_POSITIONS, K_POINTS. During computation the system followed Algorithm of Self Consistent Iteration. Self consistent iterations to solve this problem started with an initial guess of the charge density n(r), then obtained a guess for V_{ext} and solved Kohn-Sham equation for wave function ψ_i(r) to update charge density and external potential. Then, Kohn-Sham equation was solved again for the new wave function and the process was carried on until the difference between two consecutive external potential is below a certain tolerance (equivalently, the wave functions are close to stationary). Flow chart scheme of SCF to iterate Kohn-Sham equations for a set of fixed nuclear (ionic) positions is shown in the figure below.

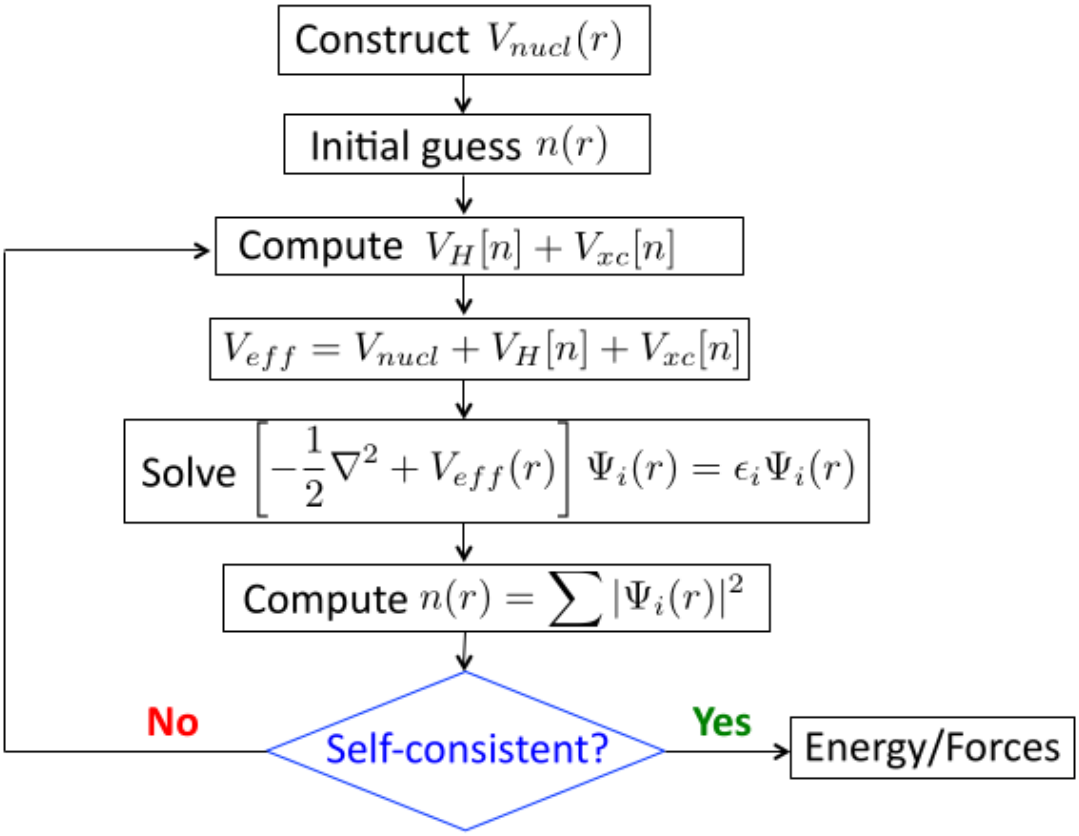

Figure 3.1: Flow chart scheme of SCF to iterate Kohn-Sham equations for a set of fixed nuclear (ionic) positions

4

Result and Discussion

4.1 Introduction

In this chapter, the structural and electronic properties of Bismuth ferrite, $BiFeO_3$ was calculated with in the frame work of the density functional theory. The important aspects in studied Bismuth ferrite are the total minimum energy and total minimum force, lattice constant, band structure and density of state of $BiFeO_3$. Results are mainly presented in figures. The first results are the total minimum energy per cell with respect to cut-off as well as k-points sampling and second results are total minimum forces values for three dimensional $BiFeO_3$ with respect to cut-off and K-points sampling. Then comes the results for the equilibrium lattice constants, band structure, density of state of $BiFeO_3$ and partial density of state. Graphs were plotted to obtain the optimized parameters for $BiFeO_3$ structure with in the Perdew-Burke-Ernzerhof (PBE) exchange-correlation functional, Vanderbilt (Optimized Norm-Conservinng) pseudopotentials and the plane wave basis set.

4.2 Total minimum energy of $BiFeO_3$ and its convergence with respect to cut-off energy

Most stable approach is to directly minimize the total energy by calculating the total energy with SCf method, we get the ground state properties. During the calculation of total minimum energy of $BiFeO_3$ with respect to cut-off energy, the only variable parameter in the input code is cutoff energy(ecutwfc) and the other parameters are kept constant. The total minimum energy of $BiFeO_3$ with respect to cut-off energy calculation is carried out for different values of cutoff energy starting from 20 Ry up

to 140 Ry in the interval of 10 Ry

Table 4.1: The calculated total minimum energy and ΔE with respect to cut-off energy

Cut-off Energy (Ry)	Total Minimum Energy (Ry)	ΔE	Cut-off Energy (Ry)	Total Minimum Energy (Ry)	ΔE
20	-486.82765897	26.93824868	90	-513.76578560	0.00012205
30	-504.25453986	9.51136779	100	-513.76582811	0.00007954
40	-510.71070478	3.05520287	110	-513.76586295	0.0000447
50	-512.90795541	0.85795224	120	-513.76587606	0.00003159
60	-513.58696733	0.17894032	130	-513.76589199	0.00001566
70	-513.74066498	0.02524267	140	-513.76590765	0.00000000
80	-513.76399164	0.00191601			

4.2.1 Convergence test of total minimum energy of $BiFeO_3$ with respect to cut-off energy

The convergence test of the total minimum energy of $BiFeO_3$ with respect to the plane wave cutoff energy was calculated. An increment of energy cut-off for wave function is made until the convergence is achieved. The total minimum energy of $BiFeO_3$ is converged at 90 Ry plane wave cutoff energy and the total ground state energy has its minimum at -513.76578560 Ry as shown in table 4.3

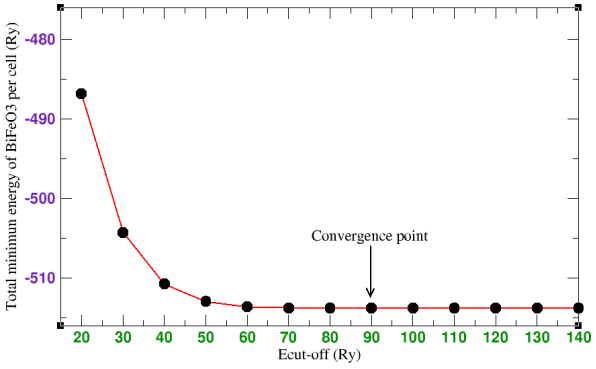

Figure 4.1: Convergence of total minimum energy of $BiFeO_3$ per cell with respect to cut-off energy

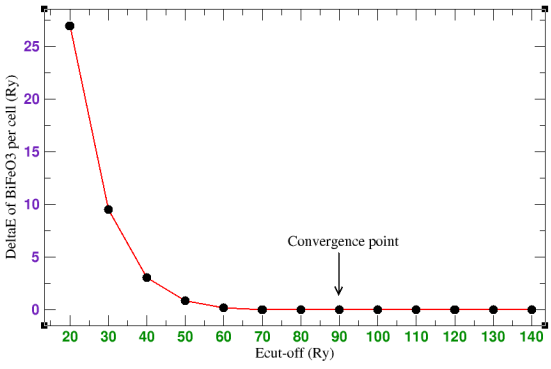

Figure 4.2: Convergence of ΔE_{tot}^{min} of $BiFeO_3$ per cell with respect to cutoff energy

4.3 Total minimum energy of $BiFeO_3$ with respect to K-points

In this case, the calculation of total minimum energy was performed using different k-point grid sizes 1x1x1 to 15x15x15 based on the convergence criteria. In this calculation the other variables: lattice constants and cutoff energy are set fixed. The calculated total minimum energy with respect to k-point grids are given in table 4.2

Table 4.2: The calculated total minimum energy and ΔE with respect to k-point grid

K-point	Total Minimum energy (Ry)	ΔE (Ry)
1x1x1	-513.00907309	-0.10141061
3x3x3	-512.90614019	0.00152229
5x5x5	-512.90795483	-0.00029235
7x7x7	-512.90795047	-0.00028799
9x9x9	-512.90739613	0.00026635
11x11x11	-512.90790420	-0.00024172
13x13x13	-512.90766479	-0.00000222
15x15x15	-512.90766248	0.00000000

4.3.1 Convergence test of total minimum energy of $BiFeO_3$ with respect to K-point sampling

A convergence test of total minimum energy of $BiFeO_3$ with respect to k-point sampling was done. The total minimum energy is converged at 5x5x5 k-point grid as shown in Figure 4.3. The total ground state energy has its minimum at -512.90795483 Ry (see table 4.2)

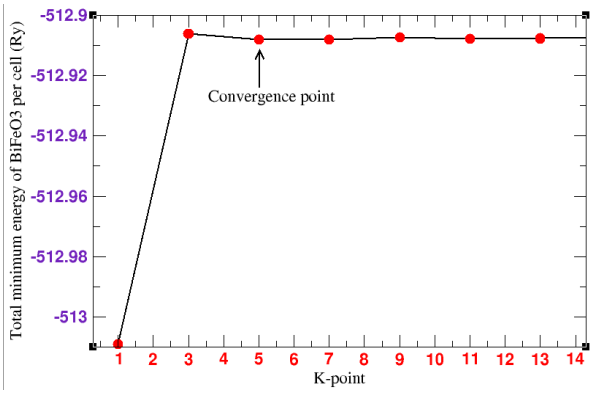

Figure 4.3: Convergence of total minimum energy of $BiFeO_3$ with respect to k-point grid

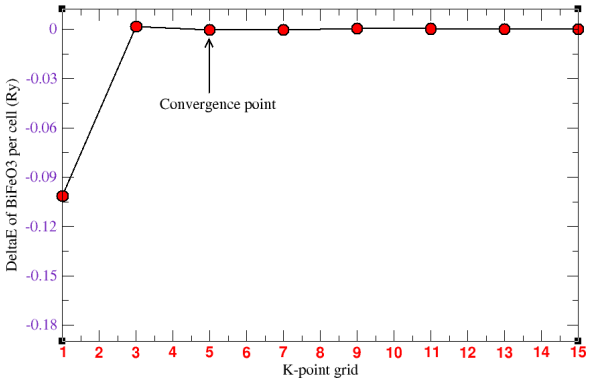

Figure 4.4: Convergence of ΔE_{tot}^{min} of $BiFeO_3$ with respect to k-point grid

4.4 The equilibrium lattice constant of $BiFeO_3$

The lattice constant of $BiFeO_3$ was determined. We used the plane wave cut-off energy and k-point grid from the convergence test of total minimum energy with respect to cut-off energy and k-point grid respectively as discussed under sections 4.2.1 and 4.3.1

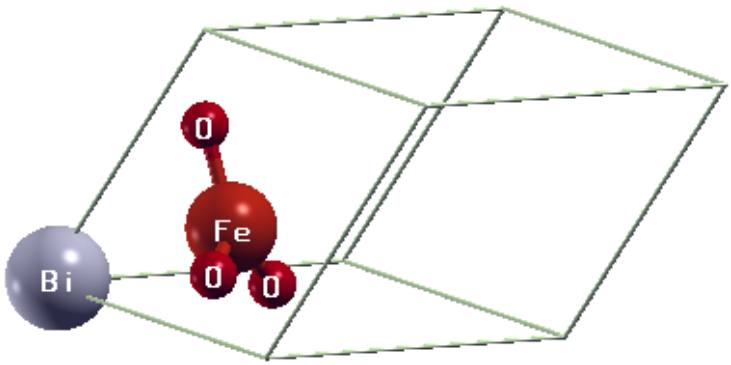

Figure 4.5: Lattice structure of $BiFeO_3$

4.4.1 Convergence test of total minimum energy of $BiFeO_3$ with respect to lattice constant

To find the equilibrium lattice constant of $BiFeO_3$ we estimated serious of lattice parameters from (9.55-10.75) with difference of 0.05 it taken and the lattice constant convergence reached at 10.0 Bohr which is the value for which we get minimum total energy and this value is used for further calculations. Finally, the total energy plotted against that lattice constant (10.25 Bohr) shown in graph below. In this calculation the energy cutoff and the K-points sampling was made fixed (90 Ry, 5×5×5 k-point) using the cut-off and k-point grid criteria for energy convergence. The numerical calculation shows that the equilibrium lattice constant is 10.0 Bohr. This result is comparable to the experimental result with percentage error of 2.4% .

Table 4.3: The calculated total minimum energy and ΔE with respect to lattice parameter

alat (bohr)	Total minimum energy (Ry)	ΔE	alat (bohr)	Total minimum energy (Ry)	ΔE
9.50	-512.85807539	-0.0088189	10.20	-512.91094305	-0.06168656
9.55	-512.86693003	-0.00768101	10.25	-512.90776429	-0.0585078
9.60	-512.87628320	-0.02702671	10.30	-512.90371351	-0.05445702
9.65	-512.88728785	-0.03803136	10.35	-512.90163013	-0.05237364
9.70	-512.89570075	-0.04644426	10.40	-512.89611436	-0.04685787
9.75	-512.89867205	-0.04941556	10.45	-512.89134063	-0.04208414
9.80	-512.90700305	-0.05774656	10.50	-512.88450938	-0.03525289
9.85	-512.90993088	-0.06067439	10.55	-512.87915167	-0.02989518
9.90	-512.91139687	-0.06214038	10.60	-512.87211741	-0.02286092
9.95	-512.91203825	-0.06278176	10.65	-512.86495779	-0.0157013
10.00	-512.915263374	-0.06600688	10.70	-512.85693750	-0.00768101
10.15	-512.91402999	-0.0647735	10.75	-512.84925649	0.00000000

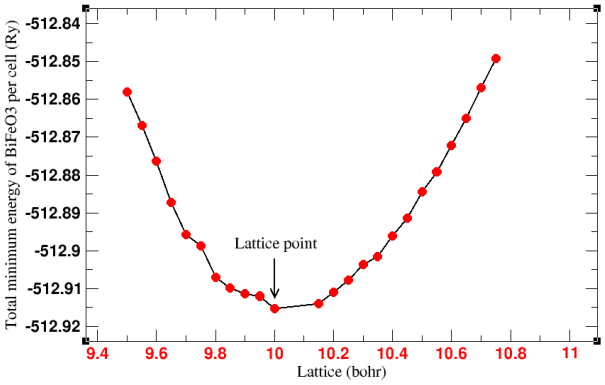

Figure 4.6: Convergence of total minimum energy of $BiFeO_3$ with respect to k-point grid

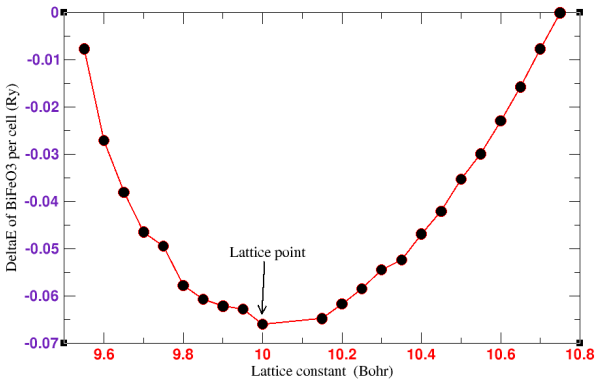

Figure 4.7: Convergence of ΔE_{tot}^{min} of $BiFeO_3$ with respect to k-point grid

4.5 Band structure of Bismuth ferrite $BiFeO_3$

The fundamental basis for understanding materials and phenomena ultimately rests upon understanding electronic structure. The band structure of $BiFeO_3$ is computed. To do this, the high symmetry path is generated using k-path selection with the help of XCrysden software as shown in the Figure 4.8. The k-path is generated by following Rhombohedral lattice high symmetry line in the Brillouin zone as indicated in : Γ-L-B1|B-Z-Γ-X| Q-F-P1-Z|L-P.

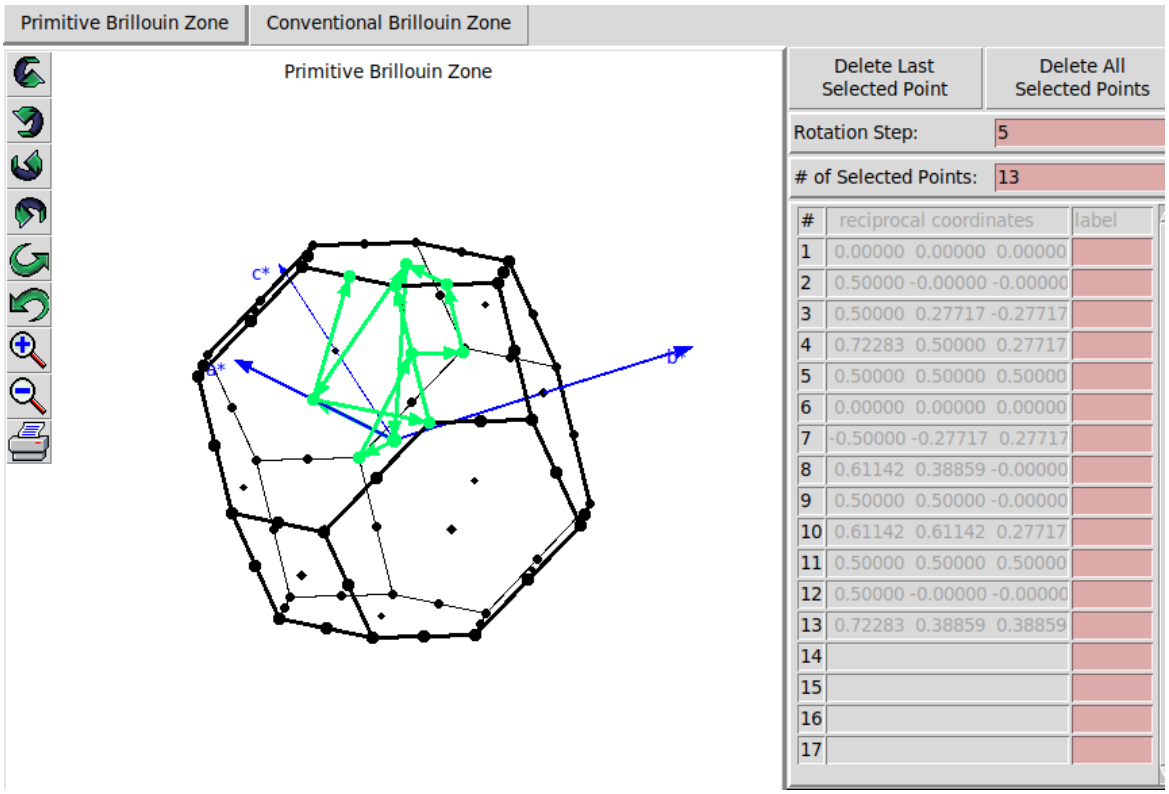

Figure 4.8: Band path selection of $BiFeO_3$ using XCrySDen

4.6 Band structure of Bismuth ferrite ($BiFeO_3$) calculations

To determine the band structure the k-points are generated along high symmetry following the k-path using xcrysden software. The energy band structure of $BiFeO_3$ is presented in Figure 4.8. Energy gap between unoccupied and occupied energy levels is among the ways that we can determine the difference between electrical properties of metals, semiconductors and insulators. The valence band is located below the Fermi level and the conduction band is located above the Fermi level. The band gap has been calculated as the difference between the energies for the minimum of the conduction band and the maximum of the valence band.

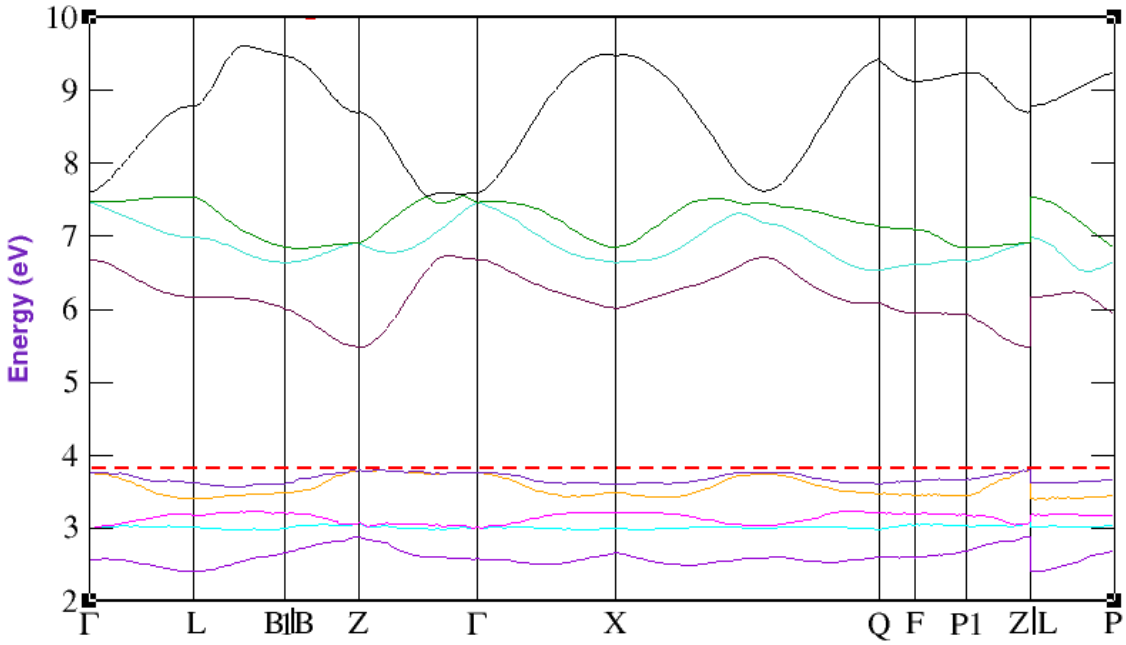

Figure 4.9: Band structure of $BiFeO_3$

4.7 Total density of states

Density of state (Dos) it is help to understand the behavior of state occupancy over specific energy intervals. It provides detail of the state which are unoccupied and the state which are occupied. The importance of analyzing density of state is to study whether the material is conductor, semiconductor or insulator. According to the plot graph the we observe that the band gap value $BiFeO_3$ categorizes it as a semiconductor material.

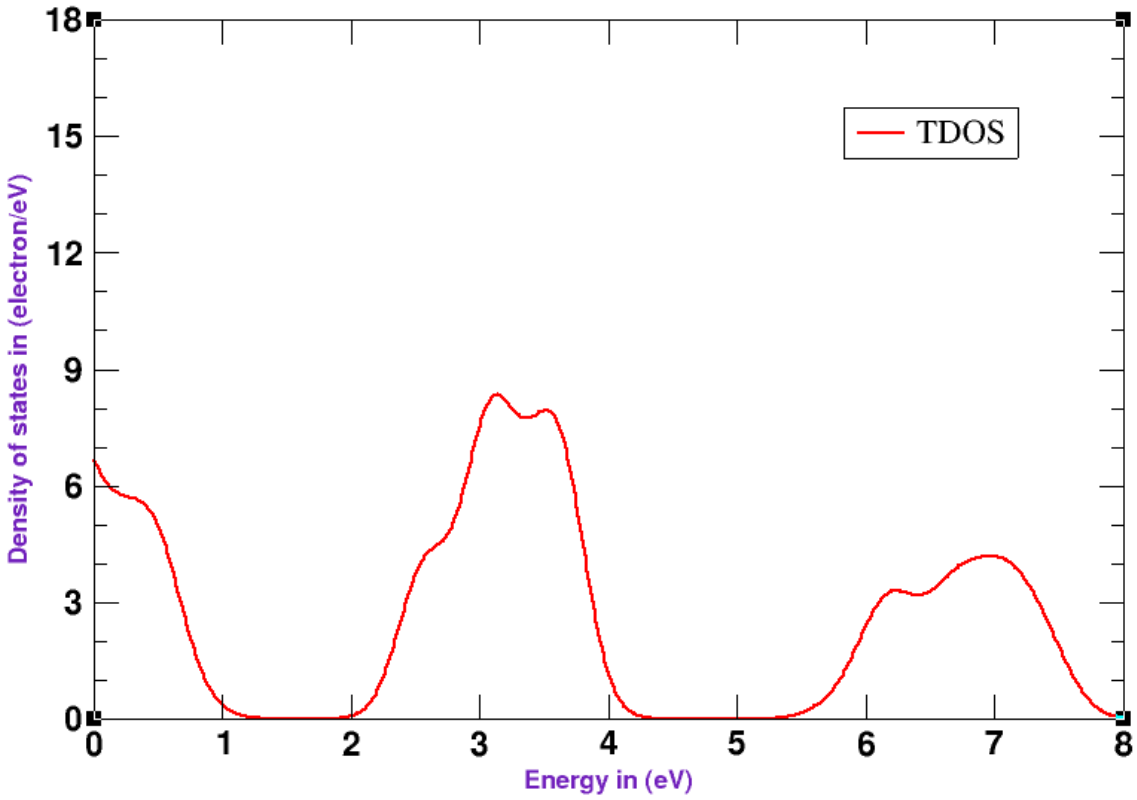

Figure 4.10: Total Density of states (TDOS) of $BiFeO_3$

4.8 Projected density of states (PDOS)

The projected density of states (PDOS) was mainly show the relative contribution of a particular atom/orbital to the total DOS. The PDOS plots also show which specific states has the highest density of states (DOS) near the valence band maximum (VBM) and conduction band minimum (CBM) in semiconductors and insulators. The Projected density of states (PDOS) of $BiFeO_3$ originate from Bi, Fe and O states. From Figure 4.11 The plot of partial density of state we verified that in orbital of Fe atom is dominant in valence band and the orbital of Bi atom is dominant in the conduction band. The state of oxygen atom has contribution both in valence band and conduction band.

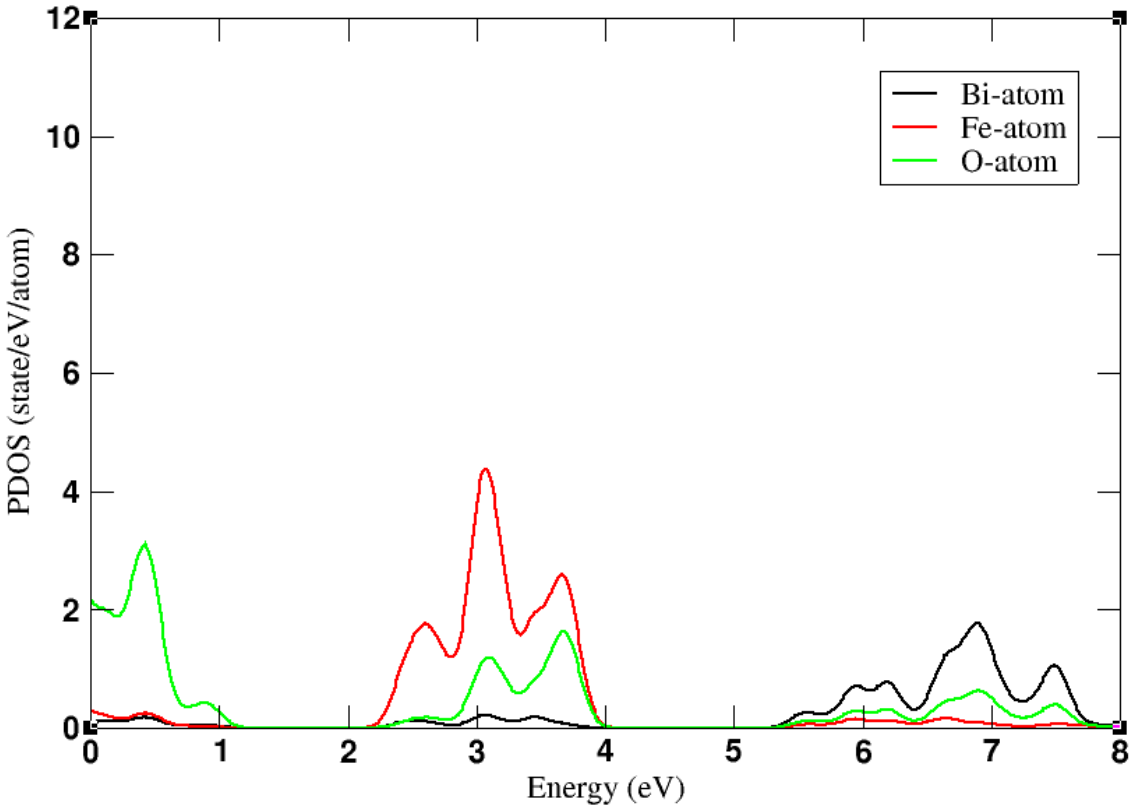

Figure 4.11: Projected Density of States (PDOS) of $BiFeO_3$

5

conclusion

In this thesis first principle calculation was used to investigate the electronic and structural properties of $BiFeO_3$. The plane wave self-consistent field (PWSCF) and norm conserving pseudopotentials with generalized gradient approximation (GGA) were implemented in Quantum Espresso package. All calculations have been carried out using Quantum Espresso package. The total minimum energy calculation was performed as a function of cut-off energy and k-point samplings. The total energy convergence test was achieved at the energy cut-off 90 Ry and at 5x5x5 k-point grid size. The total minimum energy of $BiFeO_3$ per atom is -513.76578560 Ry and -512.90795483 Ry with respect to energy cutoff and k-point grid respectively. The computational results show that the total minimum energy per atom is monotonically decreasing with increasing cut-off energy due to variational principle. However, this trend can not be predicted from increasing the k-point sampling. The theoretical lattice constant was determined and its value is 10.0 Bohr. The band structure was determined by generating k-points along high symmetry following the k-path using xcrysden software. The computed values of band gap energy using band structure of $BiFeO_3$ was 1.67 eV using density of states (DOS) of Bismuth ferrite.

The Projected density of states (PDOS) of $BiFeO_3$ originate from Bi, Fe and O states. The orbital of Fe atom is dominant in valence band and the orbital of Bi atom is dominant in the conduction band. The state of oxygen atom has contribution both in valence band and conduction band.

The importance of analyzing density of state is to study whether the material is conductor, semiconductor or insulator. According to the graph that we plot the band gap value $BiFeO_3$ categorizes it as a semiconductor material.

Bibliography

[1] M. Fiebig, J. "Revival of the Magnetoelectric Effect" Journal of Physics D: Applied Physics, **vol**.38(8),Article No.R123 - R152,(2005).
DOI:10.1088/0022-3727/38/8/R01

[2] G. Catalan, J.F. Scott, Physics and applications of bismuth ferrite ,Advanced materials ,**vol**.21(24),**pp**.2463-2485,(2009)
https://doi.org/10.1002/adma.200802849

[3] P. Fischer, M. Polomska, I. Sosnowska, M. Szymanski, J. "Temperature dependence of the crystal and magnetic structures of $BiFeO_3$" Journal of Physics C: Solid State Physics,**vol**.13(10),(1979)
DOI10.1088/0022-3719/13/10/012

[4] J.T.Heron, D.G. Schlom, R. Ramesh, "Electric field control of magnetism using BiFeO3-based heterostructures"Applied Physics Review,**vol**.1(2),(2014)
https://doi.org/10.1063/1.4870957

[5] Kubel, Frank; Schmid, Hans (1990). "Structure of a Ferroelectric and Ferroelastic Monodomain Crystal of the Perovskite BiFeO3". Acta Crystallographica. **vol**.46(6),**pp**.698–702,(1990)
doi:10.1107/S0108768190006887.

[6] Catalan, Gustau; Scott, James F."Physics and Applications of Bismuth Ferrite" (PDF).Advanced Materials.**vol**.21(24),**pp**.2463–2485,(2009).
doi:10.1002/adma.200802849.S2CID49689448.

[7] D. Varshney, A. Kumar, K. Verma, "Effect of A site and B site doping on structural, thermal and dielectric properties of $BiFeO_3$ ceram-

ics"Journal of J. Alloys Compd,**vol**.509(33),**pp**.8421-8426,(2011).
https://doi.org/10.1016/j.jallcom.2011.05.106

[8] Catalan.G and J.F. Scott, Physics and Applications of Bismuth Ferrite. Advanced Materials,**vol**.21(24),**pp**.2463-2485.(2009)
https://doi.org/10.1002/adma.200802849

[9] Rojac T., A. Bencan, B. Malic, G. Tutuncu, J.L. Jones, J.E. Daniels, and D. Damjanovic,"$BiFeO_3$ Ceramics: Processing, Electrical, and Electromechanical Properties". Journal of the American Ceramic Society,**vol**.97(7), **pp**.1993-2011,(2014)
.https://doi.org/10.1111/jace.12982

[10] Anas MM, Gopir G. "Electronic and optical properties of small hydrogenated silicon quantum dots using time-dependent density functional theory". Journal of Nanomaterials,**vol**.16(1),**pp**.325,(2015).
https://doi.org/10.1155/2015/481087

[11] J. Wang, J.B. Neaton, H. Zheng, V. Nagarajan, S.B. Ogale et al., "Epitaxial $BiFeO_3$multiferroic thin film heterostructures".Science **vol**.299(5613),**pp**.1719-1722,(2003).
https://doi.org/10.1126/science.1080615.

[12] Schmidt h, "Multi-Ferroic magnetoelectrics,Ferroelectrics",**vol**.162(1-4),**pp**.317-338,(1994).
DOI:10.1080/00150199408245120 .

[13] J. T. Heron, D.G. Schlom, R. Ramesh. "Electric field control of magnetism using $BiFeO_3$ based heterostructures". Appl.Phys. Rev.**vol**.1(2),(2014).
Doi:10.1063/1.4870957.

[14] D. Khomskii, "classifying multiferroics; Mechanisms and effects".Material Science physics 2,**vol**.20(25),(2009).
DOI:10.1103/Physics.2.20 URL:http://link.aps.org/doi/10.1103/Physics.2.20.

[15] G. Dhir, P. Uniyal, N. K. Verma. "Tactics of particle size for enhanced multiferroic properties in nanoscale Ca-doped $BiFeO_3$". Physica Status Solidi C.**vol**.14(5),(2017).
https://doi.org/10.1002/pssc.201600253

[16] J. Wang, K. Jin, H. Guo, J. Gu, Q. Wan, X. He, X. Li, X. Xu, G.Yang. "Evolution of structural distortion in $BiFeO_3$ thin films probed by second-harmonic generation".Scientific Reports,**vol**.6, Article number.38268,(2016).
Doi:10.1038/srep38268.

[17] Z. Li, Y. Wang, G. Tian, P. Li, L. Zhao et al., High-density array of ferroelectric nanodots with robust and reversibly switchable topological domain states. Science Advance,**vol**.3(8),(2017).
https://doi:10.1126/sciadv.1700919.

[18] J. Allibe, S. Fusil, K. Bouzehouane, C. Daumont, D. Sando et al., "Room temperature electrical manipulation of giant magnetoresistance in spin valves exchange-biased with $BiFeO_3$" .Nano Lett,**vol**.12(3),**pp**.1141–1145,(2012).
https://doi.org/10.1021/nl202537y.

[19] D. Kan, L. Palova, V. Anbusathaiah, C.J. Cheng, S. Fujino, V.Nagarajan, K.M. Rabe, I. Takeuchi, "Universal behavior and electric-field-induced structural transition in rare-earth-sub-stituted $BiFeO_3$" . Adv. Funct.Mater.**vol**.20(7),**pp**.1108-1115,(2010).
https://doi.org/10.1002/adfm.200902017.

[20] I. Sosnowska, T. Peterlinneumaier, E. Steichele,"Spiral magnetic ordering in bismuth ferrite $BiFeO_3$". Journal of Physics C: Solid State Physics,**vol**.15(23),**pp**.4835-4846 ,(1982).
https://DOI10.1088/0022-3719/15/23/020.

[21] J. R. Teague, R. Gerson, and W. J. James, "Dielectric hysteresis in single crystal BiFeO $_3$"Solid State Communications,**vol**.8(13), **pp**.1073-

1074,(1970).
DOI:10.1016/0038-1098(70)90262-0.

[22] Ghosh, Sushmita; Dasgupta, Subrata; Sen, Amarnath; Sekhar Maiti, Himadri "Low-Temperature Synthesis of Nanosized Bismuth Ferrite by Soft Chemical Route". Journal of the American Ceramic Society.**vol**.88(5),**pp**.1077-1365, (2005).
https://doi.10.111/j.1551-2916.2005.00306.x

[23] Chelikowsky JR. Introductory Quantum Mechanics with MATLAB: For Atoms, Molecules, Clusters and Nanocrystals. John Wiley and Sons,1^{st} edition,(2019).

[24] Kubel,Frank; Schmid, Hans (1990). "Structure of a Ferroelectric and Ferroelastic Monodomain Crystal of the Perovskite BiFeO3". Acta Crystallographica.**vol**.46(6),**pp**.698–702,(1990).
https://doi.10.1107/S0108768190006887

[25] Ryan Synk. An Introduction to Density Functional Theory and the Quantum Many-body Problem,(2021).
https://www.math.umd.edu/~mariakc/RIT_Fall2021/quantum_talk.pdf.

[26] Coleman P.Introduction to many-body physics. Cambridge University Press;1st edition,(2016).

[27] Armiento R. From exchange-correlation functional design to applied electronic structure calculations,(2022).
URN:urn:nbn:se:kth:diva-428

[28] Koch W, Holthausen MC. A chemist's guide to density functional theory 2^{nd}. John Wiley and Sons,(2001).
DOI:10.1002/3527600043

[29] Sherrill CD. An introduction to Hartree-Fock molecular orbital theory. School of Chemistry and Biochemistry Georgia Institute of Technology,(2000).

[30] Fermi E. Un metodo statistico per la determinazione di alcune priorieta dell'atome. Rend. Accad. Naz. Lincei. 6(602-607),(1927).

[31] Mahan GD, Subbaswamy KR. Local density theory of polarizability.Springer Science and Business Media,(1990).
DOIhttps://doi.org/10.1007/978-1-4899-2486-5

[32] Harrison NM. An Introduction to Density Functional.Computational materials science. (2003).

[33] Lee, June Gunn,Computational materials science :an introduction Second edition Boca Raton ,(2017).
http://www.taylorandfrancis.com http://www.crcpress.comwww.iran-mavad.com

[34] Kohn W, Sham LJ. "Self-consistent equations including exchange and correlation effects".Physical Review journals Archive. **vol**.140(4A),(1965).
DOI:https://doi.org/10.1103/PhysRev.140.A1133

[35] Hohenberg P. W. Kohn. L. J. Sham, "Inhomogenous Electron Gas" Phys.Rev. 136 A-1133 Phys. Rev.**vol**.136,**pp**.864,(1964).
https://journals.aps.org/pr/abstract/10.1103/PhysRev.136.B864

[36] Perdew JP, Zunger A. "Self-interaction correction to density-functional approximations for many-electron systems". Physical Review B.**vol**.23(10),5048,(1981).
DOI:https://doi.org/10.1103/PhysRevB.23.5048.

[37] Perdew JP, Chevary JA, Vosko SH, Jackson KA, Pederson MR, Singh DJ, Fiolhais C."Atoms, molecules, solids, and surfaces: Applications of the generalized gradient approximation for exchange and correlation"

Phys.Rev.**vol**.46,6671,(1992).
DOI:https://doi.org/10.1103/PhysRevB.46.6671

[38] Perdew JP, Burke K, Ernzerhof M. Generalized gradient approximation made simple. Physical review letters.**vol**.77(18),(1996).
DOI:https://doi.org/10.1103/PhysRevLett.77.3865

[39] Singh DJ, Nordstrom L. Planewaves, Pseudopotentials,and the LAPW method. Springer Science and Business Media,ISBN 0387296840, 9780387296845,(2006).

[40] Pickett WE. Pseudopotential methods in condensed matter applications. Computer Physics Reports,**vol**.9(3),**pp**.115-197,(1989).
DOI:10.1016/0167-7977(89)90002-6.

[41] Hung NT,Nugraha AR, Saito R. Quantum ESPRESSO Course for Solid-State Physics. CRC Press;eBook ISBN 9781003290964,(2022).
DOIhttps://doi.org/10.1201/9781003290964

[42] Zunger A, Cohen ML."First-principles nonlocal-pseudopotential approach in the density-functional formalism.II.Application to electronic and structural properties of solids". Phys.Rev.**vol**.20(10),**pp**.4082,(1979).
https://doi.org/10.1103/PhysRevB.20.4082.

[43] Sholl DS, Steckel JA. Density Functional Theory: A Practical Introduction, 2nd Edition. John Wiley and Sons; ISBN: 978-1-119-84088-6, (2022).

[44] Ashcroft NW, Mermin ND. Solid state physics.Cengage Learning (2021); ISBN 0357670817, 9780357670811,(2021)
https://www.chem.uci.edu/~lawm/AM%20Ch%208-9.pdf

[45] Monkhorst HJ, Pack JD. "Special points for Brillouin-zone integrations". Physical review B.**vol**.13(12),**pp**.5188-5192,(1976).
http://dx.doi.org/10.1103/PhysRevB.13.5188.

[46] Giannozzi P, Baroni S, Bonini N, Calandra M, Car R, Cavazzoni C, Ceresoli D, Chiarotti GL, Cococcioni M, Dabo I, Dal Corso A. QUANTUM ESPRESSO: a modular and open-source software project for quantum simulations of materials.Journal of physics.Condensed Matter:an Institute of Physics Journal,**vol**.21(39),(2009).
https://doi.org/10.1088/0953-8984/21/39/395502

[47] Perdew JP, Parr RG, Levy M, Balduz Jr JL. "Density-functional theory for fractional particle number:derivative discontinuities of the energy"Physics Review Letters.**vol**.49(23),(1982).
DOI:https://doi.org/10.1103/PhysRevLett.49.1691

[48] Troullier N, Martins JL. "Efficient pseudopotentials for plane-wave calculations". Physical Reviw. **vol**.43(3),(1991).
DOI:https://doi.org/10.1103/PhysRevB.43.1993

[49] Hohenberg P, Kohn W. "Inhomogeneous electron gas".Phys.Rev. **vol**.136(3B),**pp**.864,(1964).
https://journals.aps.org/pr/pdf/10.1103/PhysRev.136.B864

[50] Kresse G and Furthmmuller J, 1996. Efficient iterative schemes for ab initio total-energy calculations using a plane-wave basis set. Physical Rev, **vol**.54 **pp**.11169-11186,(1996).
http://dx.doi.org/10.1103/PhysRevB.54.11169.

JIMMA UNIVERSITY

COLLAGE OF NATURAL SCIENCES

PERFORMANNCE CERTIFICATE FOR MASTER'S DEGREE

Name of Student: Pal Gatluak Deng

Graduate Program: MSc Regular

ID No.: RM0715/15

1.Course Work Performance Excellent, Very Good, Good, Satisfactory, Fail.

Course Code	Course Title	Cr.hr	Score(100)	Grade	Rank	Remark
Phys 799	Graduate Thesis	6	81	A^-	Very Good	

Thesis Title:**FIRST PRINCIPLE CALCULATION OF STRUCTIONAL AND ELECTRONIC PROPERTIES OF $BiFeO_3$ USING QUANTUM ESPRESSO PACKAGE**

2. Board of Examiners decision Mark X in one of the boxes. Pass ☐ Failed ☐

If failed, give reasons and indicate plans for re-examination.

_____

_____

_____

3.Approved by:Name and Signature of members of the examining Board, and Deans,SGS

Committee member	Name	Sign	Date
Examiner	_____	_____	_____
External Examiner	_____	_____	_____
Internal Examiner	_____	_____	_____
Major Advisor	_____	_____	_____
Department Head	_____	_____	_____

School of Graduate Studies

Jimma University

College of Natural Sciences

MSc. Thesis Approval Sheet

We the undersigned, member of the Board of Examiners of the final open defense by Pal Gatluak Deng have read and evaluated his thesis entitled **FIRST PRINCIPLE CALCULATION OF STRUCTIONAL AND ELECTRONIC PROPERTIES OF $BiFeO_3$ USING QUANTUM ESPRESSO PACKAGE** and examined the candidate. This is therefore to certify that the thesis has been accepted in partial fulfillment of the requirements for the degree Master of Science in Physics (Condensed Matter Physics).

Committee member	Name	Sign	Date
Examiner	_____	_____	_____
External Examiner	_____	_____	_____
Internal Examiner	_____	_____	_____
Major Advisor	_____	_____	_____
Department Head	_____	_____	_____

School of Graduate Studies

Graduate Thesis Ownership Agreement

This thesis is a property of Jimma University, an institution that awarded MSc Degree to the graduate student and funded its research cost fully or partly. The research work was accomplished under the close support and supervision of the assigned university's academic staff. It is therefore strictly forbidden to publish, modify or communicate to or put at the disposal of third party the entire document or any part there of with out the common consent of the research supervisor(s) and the graduate. Disregarding this agreement would lead to accountability according to the Jimma university's Research and publication Misconduct policy Article 1.7 of the university's Document for "Guidelines and procedures for Research, June 2024".

Name of Graduate student	Signature	Date
Pal Gatluak		

Name of the Research Supervisor	Signature	Date
Prof. Menberu Mengesha (PhD)		

Thesis Title: FIRST PRINCIPLE CALCULATION OF STRUCTIONAL AND ELECTRONIC PROPERTIES OF $BiFeO_3$ USING QUANTUM ESPRESSO PACKAGE

Degree Awarded: **(MSc)**